

On-Surface Synthesis of Sandwich Molecular Nanowires on Graphene: Supporting Information

Felix Huttmann,^{1,*} Nicolas Schleheck,¹ Nicolae Atodiresei,² and Thomas Michely¹

¹*II. Physikalisches Institut, Universität zu Köln, Zùlpicher Straße 77, 50937 Köln, Germany*

²*Peter Grünberg Institute and Institute for Advanced Simulation, Forschungszentrum Jùlich, 52428 Jùlich, Germany*

(Dated: July 17, 2017)

This Supporting Information describes the growth morphologies obtained under different preparation conditions, the thermal stability and thermal decomposition behavior, and growth on hexagonal boron nitride.

GROWTH MORPHOLOGIES UNDER VARIOUS PREPARATION CONDITIONS

We have investigated the growth of EuCot on graphene using five different preparation recipes that we labeled (a) to (e), as shown in Fig. S1. Remarkably, EuCot nanowires form in all cases where Cot and Eu can meet on the surface, regardless of the deposition temperature (20 K or 300 K) and deposition order (simultaneous, Cot first, or Eu first). However, each recipe results in a different morphology of the growth, and each of these morphologies yields insights, as will be discussed in the following. The amount of Eu is the same in all cases at 0.44 monolayer (ML) Eu. 1 ML of Eu here is defined as corresponding to one layer of Eu in the $(\sqrt{3} \times \sqrt{3})R30^\circ$ superstructure, which Eu forms on graphene.

In recipe (a), a layer of Cot with a thickness on the order of 10 ML is firstly deposited onto the cold sample, at $T = 20$ K. Subsequently, Eu is deposited, and only then the sample is warmed up to room temperature. As seen in Fig. S1 (a), this results in a disordered, spaghetti-like growth mode. This is explained as follows: At 20 K, mobility of both the Cot molecule and the Eu atoms is likely frozen. The reaction between Eu and Cot therefore will take place during the warm-up from 20 K to room temperature as soon as a temperature is reached where the mobility becomes high enough. However, once Eu and Cot have reacted into nanowires in the first best and thus chaotic way, the wires cannot separate and rejoin with the available thermal energy even at room temperature. Therefore the arrangement is frozen in.

In recipe (b), graphene was first intercalated with Eu to saturation by sufficiently long deposition at a sample temperature of 700 K¹. Then, an amount corresponding to 0.44 ML Eu was deposited onto the sample at 300 K. This results in the formation of hexagonal, mostly single-layer islands of Eu on top of graphene as seen in Fig. S2 (a). Upon exposure of these islands to a Cot excess, the coverage of the islands expands from ≈ 0.44 ML to ≈ 0.66 ML, as seen in Fig. S2 (b). The monolayer-high islands are now completely composed of EuCot wires as seen in Fig. S1 (b). The structures on top of the monolayer-high islands are much less well-ordered, but consist of nanowires, too. This proves that even when Eu is already

present in the form of compact metal islands, the reaction with Cot is able to break the metal-metal bond to form EuCot.

That all Eu deposited onto graphene at room temperature (without Cot) arranges into extended hexagonal islands is only the case if the graphene has been previously fully intercalated with Eu. Deposition of Eu onto only partially or non-intercalated graphene instead yields small and mobile Eu clusters in equilibrium with islands^{2,3}.

Thus to compare, we also deposited 0.44 ML Eu at 300 K and subsequently a Cot excess just as in recipe (b), but this time, on non-intercalated graphene. The morphology as shown in Fig. S1 (c) is then indeed very different. The nanowires are now arranged in elongated crystallites, a shape clearly unrelated to the morphology of the Eu adsorption, which we attribute to the mobility of Eu during the growth.

To increase the mobility of Eu during deposition even further, we should make Eu available on the surface as atoms, rather than as clusters. To do so, we simultaneously expose the sample to Cot and Eu vapors, so that the reaction will occur before the clustering of the Eu metal. We have opened the Cot dosing valve always before and closed it after the shutter to the Eu evaporator, so that there is not only more Cot than Eu in total, but also at every single point in time. Without Eu intercalation, this is the recipe (d) shown in Fig. S1 (d), which is the one that is also shown in Fig. 2 and 5 (a) of the main paper. We observe that the crystallites have become much larger, indicating a reduced nucleation density, in line with our expectations. The defect density is also reduced, because Eu in metal clusters does not have to rearrange into Eu-Cot islands, but rather the EuCot islands can grow by direct incorporation of Eu adatoms.

Fig. S1 (e) is an STM topograph obtained when graphene is first intercalated with Eu to saturation, and afterwards simultaneously exposed to 0.44 ML Eu and Cot vapor as before. In contrast to recipe (d), small areas of a second layer of nanowire bundles on top of the first layer have formed as indicated by the arrows in Fig. S1 (e). This is despite the fact that the first layer is not completed at this coverage. Nanowires in the second layer lie mostly parallel to the first layer. Whether and at which coverage a second layer tends to form before completion of the

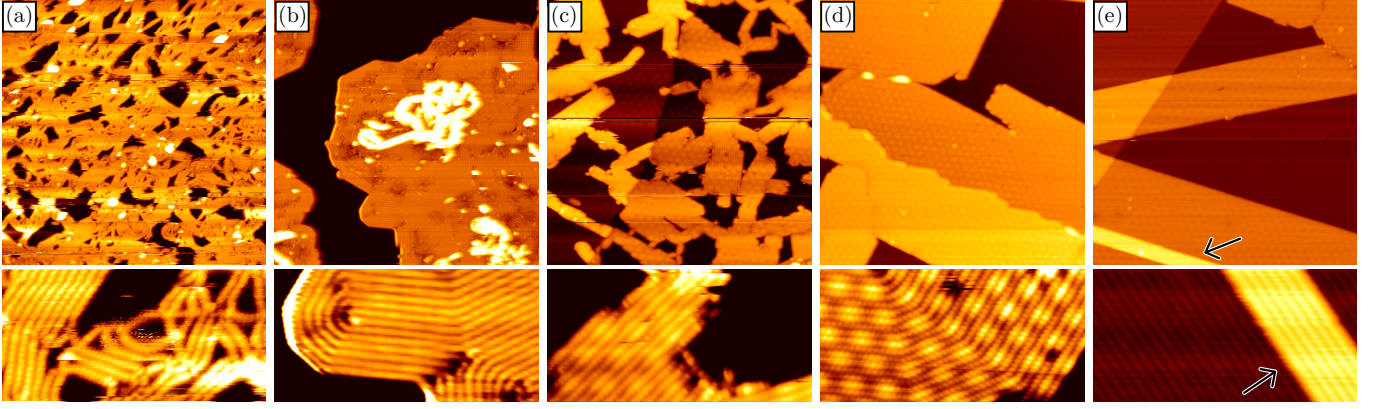


FIG. S1. STM topographs of EuCot nanowires formed under five different preparation conditions, see text. Image size top row: $(82 \text{ nm})^2$. Bottom row: $20 \text{ nm} \times 10 \text{ nm}$.

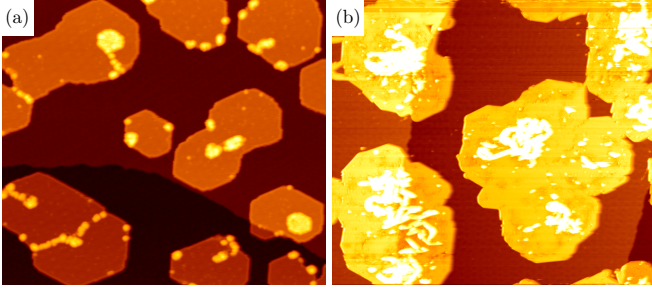


FIG. S2. STM topographs of Eu deposited onto Eu-intercalated graphene at room temperature (a) before exposure to Cot vapor (b) after exposure to Cot vapor. Image size: $164 \text{ nm} \times 144 \text{ nm}$.

first layer is a typical question in microscopic investigations of thin film growth (*e.g.*, Ref. 4). In our case, we explain the higher tendency of EuCot to form a second layer on Eu-intercalated compared to non-intercalated graphene by the energetics of the adsorption of Eu atoms: The binding energy of a Eu atom on Eu-intercalated graphene is significantly lower than the binding energy on non-intercalated graphene, a result of the ionic bonding character and resulting charge transfer³. If a Eu atom binds more strongly to graphene, it is more likely to reside there while waiting to react with a Cot molecule, and the formation of a second layer, which presumably requires the presence of Eu atoms on top of the nanowire islands, will be inhibited. We thus explain the stronger tendency toward multilayer formation on Eu-intercalated graphene as a kinetic effect during growth.

TEMPERATURE STABILITY

To assess the thermal stability of the wire bundles, we have grown EuCot at room temperature and annealed

to successively higher temperatures. Figure S3 shows STM topographs before [Fig. S3 (a)] and after stepwise annealing for 3 minutes at the indicated temperatures [Fig. S3 (b) to (f)]. Imaging was performed after cool-down to room temperature in all cases.

Annealing at 600 K [Fig. S3 (b)] leaves the wire bundle structure mostly intact. Only at the edges of the islands, what seems like small wire segments sticks out. More of this is seen at 650 K [Fig. S3 (c)]. The small wire segments detached from the islands form a network-like structure, where usually three nanowire segments meet in one point.

Annealing at 700 K [Fig. S3 (d)] destroys the ordered nanowire carpets, although a certain texture still seems to hint at the original orientation of the wires. The temperature where we observed decomposition to start is thus somewhat lower than the $500^\circ\text{C} \hat{=} 773 \text{ K}$ value given by Ref. 5 for bulk EuCot obtained by their solution method. It is plausible that the dense packing of nanowires in a 3D structure leads to a stabilization compared to nanowires in a 2D carpet on a surface, especially considering that the decomposition of the 2D carpets appears to start at the edges. No desorption of Cot was observed as discussed below.

Annealing at 800 K leads to complete decomposition as seen in Fig. S3 (e). We identify the following structures on the sample and marked them in the figure: (1) protrusions of almost uniform shape and a typical height of 3 \AA arranged in the moiré lattice; (2) clusters of typically around 10 \AA height with irregular shapes; (3) stripes and small islands of a height of about 2 \AA . The nature of (1) and (2) is unclear to us, while (3) is easily attributed to Eu which has intercalated underneath the graphene sheet⁶, as the decomposition of nanowires releases the Eu.

Annealing at 1200 K [Fig. S3 (f)] makes (1) and (2) disappear, while the amount of intercalated Eu seems to have increased. The irregularities in the pattern of intercalated Eu indicate a defective graphene layer (compare with Ref. 1, Fig. 3). In addition to the Eu intercalation islands, a

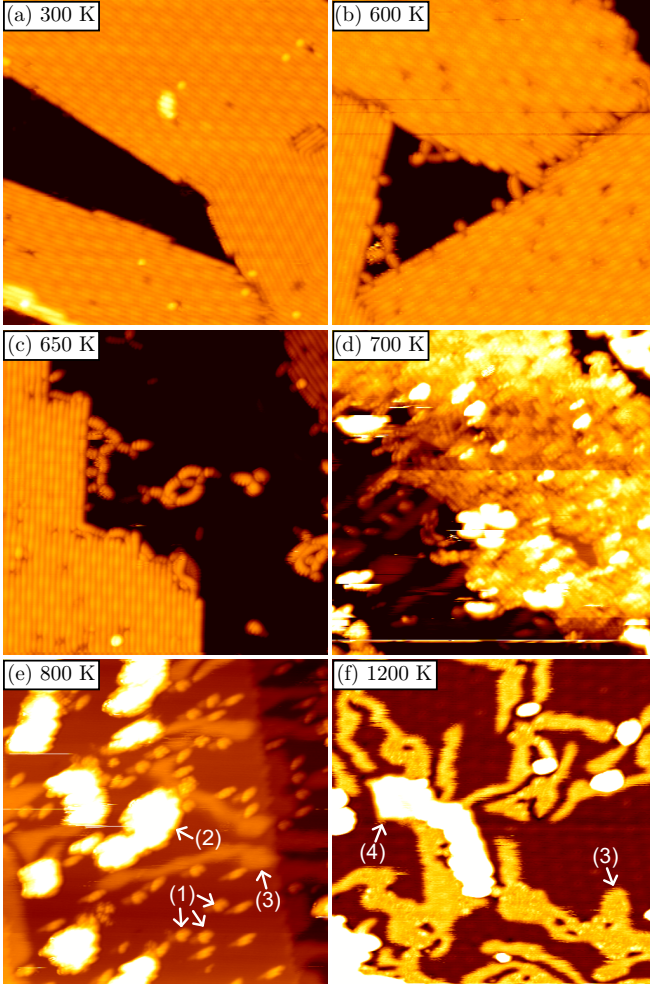


FIG. S3. STM topographs of nanowire crystallites formed by simultaneous exposure on non-intercalated graphene at room temperature [(a)], and subsequently stepwise annealed to the indicated temperatures [(b-f)]. Image size: $(41 \text{ nm})^2$. Note that (d) suffers from a double-tip artifact. For an explanation of numbers (1)–(4), see text.

new type of island appears, marked (4) in Fig. S3 (f), with a height of roughly 5.5 \AA . We suspect that this structure consists of a bilayer of graphene intercalated with one layer of Eu, as $(5.5 \text{ \AA} - 2 \text{ \AA}) \approx 3.35 \text{ \AA}$ approximately corresponds to the distance between two graphene layers in graphite.

In order to test whether Cot desorbs in molecular form from the sample during the decomposition, we have placed the sample under a mass spectrometer and monitored the signal at a mass-to-charge ratio of $m/q = 104 e/u$, corresponding to singly ionized Cot, while applying a heating ramp with a few Kelvin per second. No signal was observed, indicating that Cot does not desorb in molecular form. This is consistent with the bilayer graphene found after annealing to 1200 K and clusters of carbonaceous material if some or all of the carbon deposited on the

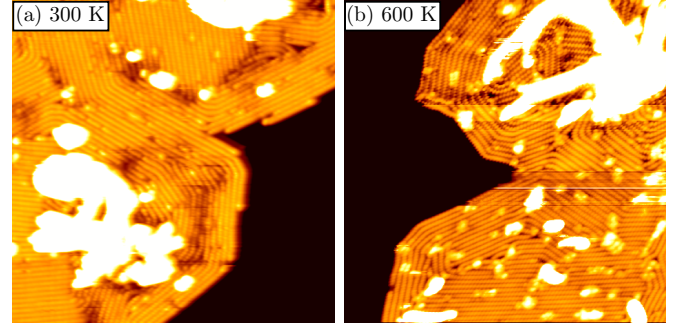


FIG. S4. STM topographs of nanowire islands formed by evaporation of Eu onto Eu-intercalated graphene and subsequent exposure to Cot at room temperature [*i.e.*, as in Fig. S1 (b)]. (a): Before annealing. (b): After annealing to 600 K. Image size: $(41 \text{ nm})^2$.

sample in the form of Cot does not desorb during heating.

One could imagine that the nanowire islands are actually not stable up to 600 K, but rather, that they dissolved during heating and re-assembled during cool-down, and thus appear unchanged when imaged again at 300 K. The fact that different growth morphologies can be produced as shown in Fig. S1 allows us to test this hypothesis: If the wires dissolved during heating, then there is no reason why the morphology after annealing should be the same as before annealing; in fact, the morphology after annealing should be independent of what was before, because the islands after annealing would always condense from the same “fluid” high-temperature phase. In Fig. S4, we compare the morphology obtained as in Fig. S1 (b), before [Fig. S4 (a)] and after [Fig. S4 (b)] annealing to 600 K, just below the onset of decomposition. It is seen that the morphology after annealing is very similar to before annealing, and at the same time very different from another morphology annealed to the same temperature as seen in Fig. S3 (b). In particular, islands in Fig. S3 (a) and (b) have longer straight edges than the islands of Fig. S4 (a) and (b), and the wires themselves are also mostly straight for the former and convoluted for the latter. Based on these observations, we exclude dissolution of islands before decomposition.

GROWTH ON HEXAGONAL BORON NITRIDE

A h-BN monolayer is isostructural and isoelectronic to graphene, however, in contrast to graphene it is a good insulator. Therefore, h-BN may be a better substrate if one would want to study the electronic structure by scanning tunneling spectroscopy or even the transport properties of the nanowire carpets. Figure S5 shows the result of the exposure of h-BN/Ir(111) to Eu and Cot vapor, using the same parameters as in the experiment on graphene shown in Fig. S1 (d) and Fig. 2 of the main paper. We can

observe that also in the case of h-BN, nanowire crystallites grow. However, the crystalline quality is significantly worse in the case of h-BN. For example, the typical size of a nanowire crystallite is on the order of 10 to 20 nm for h-BN, but is 50 to 100 nm for graphene. Possibly, this is related to the stronger interaction of h-BN with the Ir(111) surface compared to graphene, which leads to a higher corrugation and a more chemisorbed binding character of h-BN to Ir(111)⁷, and could be remedied by using a more weakly interacting substrate for h-BN, such as Cu or Ag(111)^{8–10}.

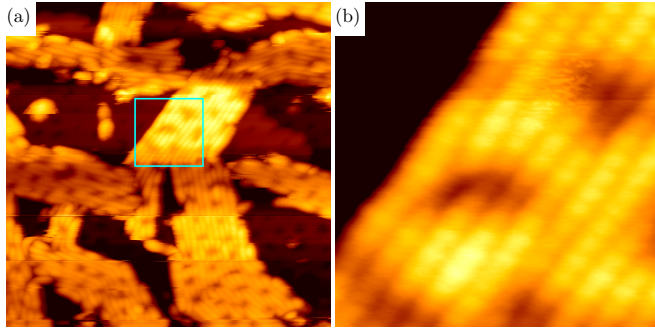


FIG. S5. STM topographs of nanowire crystallites formed by simultaneous exposure on hexagonal boron nitride. (b) is a zoom into the area in (a) indicated by the square. Image size: $(41 \text{ nm})^2$, zoom-in $(7 \text{ nm})^2$.

* huttmann@ph2.uni-koeln.de

- [1] Schumacher, S.; Huttman, F.; Petrović, M.; Witt, C.; Förster, D. F.; Vo-Van, C.; Coraux, J.; Martínez-Galera, A. J.; Sessi, V.; Vergara, I.; Rückamp, R.; Grüninger, M.; Schleheck, N.; Meyer zu Heringdorf, F.; Ohresser, P.; Kralj, M.; Wehling, T. O.; Michely, T. *Phys. Rev. B* **2014**, *90*, 235437.
- [2] Förster, D. F.; Wehling, T. O.; Schumacher, S.; Rosch, A.; Michely, T. *N. J. Phys.* **2012**, *14*, 023022.
- [3] Schumacher, S.; Wehling, T. O.; Lazić, P.; Runte, S.; Förster, D. F.; Busse, C.; Petrović, M.; Kralj, M.; Blügel, S.; Atodiresei, N.; Caciuc, V.; Michely, T. *Nano Lett.* **2013**, *13*, 5013–5019.
- [4] Schmid, A. K.; Kirschner, J. *Ultramicroscopy* **1992**, *42-44*, 483–489.
- [5] Hayes, R. G.; Thomas, J. L. *J. Am. Chem. Soc.* **1969**, *91*, 6876–6876.
- [6] Schumacher, S.; Förster, D. F.; Rösner, M.; Wehling, T. O.; Michely, T. *Phys. Rev. Lett.* **2013**, *110*, 1–5.
- [7] While the work of Schulz *et al.*¹¹ gives a peak-to-peak corrugation of $\approx 0.4 \text{ Å}$ for h-BN/Ir(111), about the same as found for graphene/Ir(111)^{12,13} and thus indicating a similar strength of interaction with the substrate, recent investigations of Farwick zum Hagen *et al.*¹⁴ point to a much stronger corrugation of h-BN/Ir(111).
- [8] Joshi, S.; Écija, D.; Koitz, R.; Iannuzzi, M.; Seitsonen, A. P.; Hutter, J.; Sachdev, H.; Vijayaraghavan, S.; Bischoff, F.; Seufert, K.; Barth, J. V.; Auwärter, W. *Nano Lett.* **2012**, *12*, 5821–5828.
- [9] Müller, F.; Hüfner, S.; Sachdev, H.; Laskowski, R.; Blaha, P.; Schwarz, K. *Phys. Rev. B* **2010**, *82*, 113406.
- [10] Laskowski, R.; Blaha, P.; Schwarz, K. *Phys. Rev. B* **2008**, *78*, 045409.
- [11] Schulz, F.; Drost, R.; Hämmäläinen, S. K.; Demonchaux, T.; Seitsonen, A. P.; Liljeroth, P. *Phys. Rev. B* **2014**, *89*, 235429.
- [12] Hämmäläinen, S. K.; Boneschanscher, M. P.; Jacobse, P. H.; Swart, I.; Pussi, K.; Moritz, W.; Lahtinen, J.; Liljeroth, P.; Sainio, J. *Phys. Rev. B* **2013**, *88*, 201406.
- [13] Busse, C.; Lazić, P.; Djemour, R.; Coraux, J.; Gerber, T.; Atodiresei, N.; Caciuc, V.; Brako, R.; N'Diaye, A. T.; Blügel, S.; Zegenhagen, J.; Michely, T. *Phys. Rev. Lett.* **2011**, *107*, 036101.
- [14] Farwick zum Hagen, F. H.; Zimmermann, D. M.; Silva, C. C.; Schlueter, C.; Atodiresei, N.; Jolie, W.; Martínez-Galera, A. J.; Dombrowski, D.; Schröder, U. A.; Will, M.; Lazić, P.; Caciuc, V.; Blügel, S.; Lee, T.-L.; Michely, T.; Busse, C. *ACS Nano* **2016**, *10*, 11012–11026.